RSC Advances

PAPER

View Article Online
View Journal | View Issue

Cite this: *RSC Adv.*, 2021, **11**, 10194

Synthesis of Gd/N co-doped ZnO for enhanced UV-vis and direct solar-light-driven photocatalytic degradation†

Hamdah S. Alanazi, Naushad Ahmad and Fahad A. Alharthi *

Received 21st December 2020
Accepted 3rd March 2021

DOI: 10.1039/d0ra10698d

rsc.li/rsc-advances

The construction of a UV-Vis and direct sunlight functioning photocatalyst is a puzzling task for organic pollutant removal. Herein, we have fabricated Gd/N co-doped ZnO nanoparticles for the first-time using a simple co-precipitation method for photocatalytic degradation application. The heteroatom doping enhances the light absorption ability and acts as a photo-induced electron–hole separator by creating a trap state. Co-doped ZnO shows comparatively high photocatalytic degradation efficiency of about 87% and 93% under UV-Vis and direct solar light respectively. Moreover, the prepared photocatalyst exhibits excellent stability for the recycling process. Hence, we believe that this heteroatom co-doped ZnO photocatalyst is an auspicious material for the photocatalytic organic pollutant degradation reaction.

1. Introduction

Over the last few years, semiconductor-based photocatalysts for organic pollutant degradation have become an attractive research area due to being cost-effective and environmentally friendly. In a photocatalytic reaction, waste pollutants are oxidized with the aid of semiconductor nanoparticles under UV or visible-light irradiation.[1] Compared to other conventional wastewater treatment methods, photocatalysis is considered the best approach to degrade organic waste without any toxic by-products. Besides, semiconductor-based photocatalyst usage was extended to degrade the inorganic and microbial-pollutants from wastewater.[2] Among various semiconducting metal oxide photocatalysts, ZnO is a widely studied photocatalyst due to its non-toxic nature, and excellent electrical, optical, and oxidation-resistant properties.[3] ZnO (n-type semiconductor) has a wide band gap of 3.4 eV with a large excitation binding energy (60 meV) value at ambient temperature. Moreover, ZnO has a higher quantum efficiency compared to TiO_2 in certain cases.[4] Though it has several advantages, the commercialization of ZnO is still affected by low photocatalytic performance, low light absorption ability, and a high rate of electron–hole recombination. To tackle these disadvantages of ZnO, several methods for example metal, non-metal doping, making the heterojunction with other semiconductors are used to improve the photocatalytic efficiency.[5]

Rare earth metal ion doping is an effective way to enhance the ZnO photocatalytic efficiency by creating the impurity level in the forbidden energy gap. In addition to this, rare-earth elements can create the trap state in ZnO crystal to reduce the electron–hole recombination rate.[6] Several rare-earth metals like Gd, La, Sm, and Yt are used as doping ions with ZnO to enrich the photocatalytic degradation efficiency. Among various rare earth metals, Gd has received great attention due to partially filled f-orbital, which is beneficial for improving the ZnO photocatalytic degradation process.[7–12]

Further, photocatalytic degradation efficiency was improved by doping the non-metals to ZnO in addition to the metal ions. The non-metal doping preferred for narrowing the bandgap of ZnO. Combination of N 2p and O 2p states aids in narrowing the bandgap of the semiconductor and resulting in the higher absorption in the visible light region. Furthermore, the existence of an N atom in the ZnO nanoparticles can advance the charge carrier transportation, enhance the specific surface area, and constrains the charge carrier's recombination rate.[13–16] Rimzhim Gupta *et al.* reported that Cu and N co-doped ZnO prepared by combustion and hydrothermal methods exhibited the better photocatalytic inactivation of *E. coli* bacteria under UV and visible light illumination.[13] Mahesh Dhonde *et al.*, reported the Cu and N co-doped TiO_2 photoanode shows 11.70% of power conversion efficiency in dye-sensitized solar cell application.[14]

Inspired by the above-mentioned literature reports, herein we have presented the Gd and N co-doped ZnO nanoparticle for photocatalytic organic pollutant degradation under UV-Vis and direct solar light irradiation for the first time. The prepared pure and co-doped ZnO photocatalysts were well analyzed through various analytical characterization techniques to know the crystallite, morphological, vibrational, and optical properties. The prepared Gd and N co-doped ZnO exhibit the enhanced light absorption ability and improved photocatalytic degradation efficiency. Reactive oxygen radicals for the photocatalytic process and constancy of the prepared nanoparticles were examined by elemental trapping and reutilize experiments.

Department of Chemistry, College of Science, King Saud University, Riyadh 11451, Kingdom of Saudi Arabia. E-mail: fharthi@ksu.edu.sa

† Electronic supplementary information (ESI) available. See DOI: 10.1039/d0ra10698d

2. Experimental

2.1. The synthesis procedure of Gd, N doped ZnO

Wet chemical co-precipitation method was used to prepare the pure, doped and co-doped ZnO nanoparticles. In brief, 5 mmol of zinc nitrate hexahydrate was dissolved in 50 ml of de-ionized water until the clear solution was obtained. Followed by 3 mol% of gadolinium nitrate and 0.5 g of melamine was added in the above solution. Then 2 g of NaOH (sodium hydroxide pellet) was added to the solution to form the precipitate. Followed by the precipitate was washed with ethanol and de-ionized water for numerous times and dried at 80 °C for 5 h in a hot-air oven. The dried powder was calcined at 500 °C for 2 h with a ramp rate of 10 °C min^{-1}. The obtained sample was crushed with the help of an agate mortar and washed three times with ethanol to remove the residual carbon waste. Then the sample was named as Gd/N/ZnO. The similar process was followed for Gd/ZnO and N/ZnO exclude the addition of melamine and gadolinium nitrate correspondingly.

2.2. Characterization

Powder X-ray diffraction analysis of the synthesized photocatalysts was analysed through BRUKER USA D8 Advance, Davinci powder X-ray diffractometer. The surface nature of the nanoparticles was examined by FESEM (Thermoscientific Apreo S) and HRTEM (JEOL, JSM-2100plus) microscopes. The optical behaviour was studied by a Shimadzu UV3600+ spectrometer (UV-DRS) and HORIBA Fluorolog (PL). The surface elements confirmation of the nanoparticles was carried out by PHI Versaprobe III. The FTIR spectrum of the synthesized nanoparticles were examined using a SHIMADZU, IRTRACER-100 with KBr mode.

2.3. Photocatalytic degradation test

Methylene blue was chosen as a target pollutant to investigate the photocatalytic degradation efficiency of the prepared nanoparticles. Homemade, pyrex glass reactor (250 ml capacity) was used for photocatalytic degradation process. In typical, 100 mg of photocatalysts was added in 100 ml of (10 mg L^{-1}) MB dye solution. The photocatalytic degradation process was carried out under 300 W halogen lamp (UV-Vis lamp) (84 319 lux) and direct sunlight (November 2020 in the period of 1 p.m to 2 p.m) (97 871 lux) irradiation. Initially, the dye solution and photocatalysts were stirred for 30 min under the dark condition to attain the adsorption–desorption equilibrium. At a regular interval of time, 3 ml of dye solution was taken out and examined by UV-Vis spectroscopy with an absorption maximum of 664 nm.

3. Results and discussion

3.1. X-ray diffraction analysis

The crystalline structure of the prepared photocatalysts was studied by powder XRD analysis and the recorded patterns were displayed in Fig. 1. From the diffraction results, it was confirmed that all the samples have an analogous diffraction pattern and it is compatible with the standard JCPDS card (36-1451) and former literature result.[3] The diffraction planes (110), (002), (101), (102), (110), (103), and (112) related to ZnO

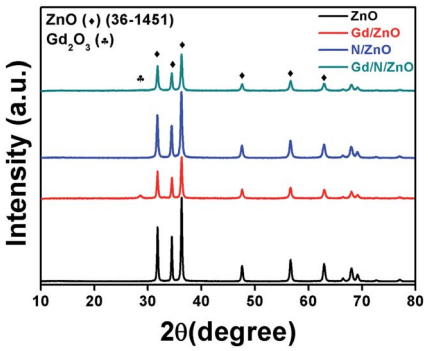

Fig. 1 XRD patterns of pure and doped ZnO nanoparticles.

nanoparticles have the 2θ values of 31.81, 34.47, 36.32, 47.61, 56.66, 62.91 and 68.04° respectively. Gd doped ZnO shows the relatively low intense XRD peaks, which revealed the doping of Gd ions reduces the crystallinity of ZnO. Moreover, the new peak positioned at 28.63° related to the Gd_2O_3 and this is well-matched with the previous report.[12] There is no peak shift and new peaks were observed at N doped ZnO nanoparticle, which demonstrated N doping have not affected the ZnO crystal system.[17] The diffraction pattern of Gd and N co-doped ZnO shows lower intensity compared to pure and N doped ZnO, which revealed the Gd^{3+} doping reduces the crystallinity and it is similar to Gd doped ZnO. Moreover, the diffraction peaks of Gd/N/ZnO shows the slight shift towards lower angle side compared to pure ZnO, which revealed that Gd^{3+} ions are interstitially doped between the ZnO lattice planes. This interstitial doping leads to increases in the lattice space of ZnO.[12]

3.2. FTIR analysis

The vibrational behaviour of the functional groups which are presented in the prepared nanoparticles were inspected by FTIR analysis. The transmittance FTIR spectra of the pure and co-doped ZnO nanoparticles were shown in Fig. 2. Pure ZnO showed the FTIR peak positioned at 420 cm^{-1} related to the lattice oxygen and metal (Zn–O) bond. The FTIR spectrum associated to the metal–oxygen bond in Gd doped ZnO was broaden compared to pure ZnO. This result demonstrated the lattice-distortion in metal–oxygen bonding due to the presence of Gd ion

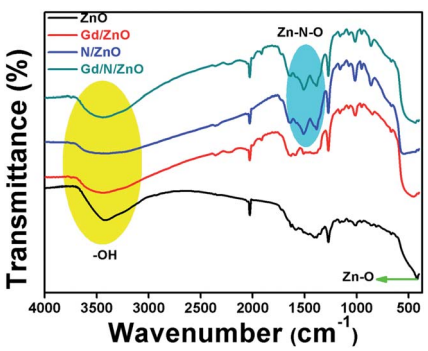

Fig. 2 FTIR spectra of pure and doped ZnO nanoparticles.

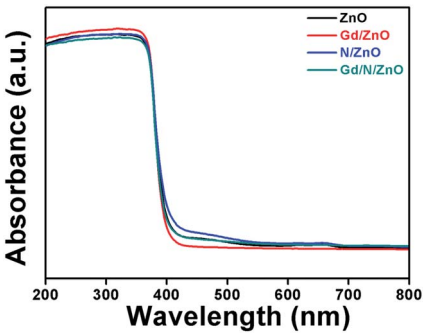

Fig. 3 UV-Vis-DRS absorption spectra of pure and doped ZnO nanoparticles.

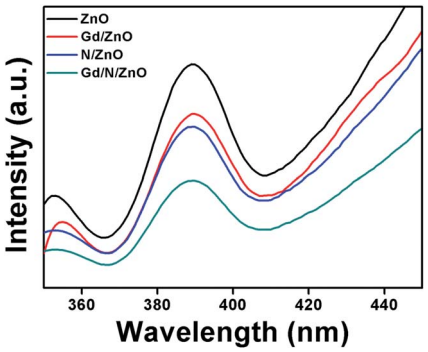

Fig. 4 Photoluminescence spectra of pure and co-doped ZnO nanoparticles.

doping.[12] N doped ZnO has the FTIR peaks positioned at 1385 and 1513 cm^{-1} attributed to stretching vibration of Zn–N and N–Zn–O bond respectively. This result provides the evidence for incorporation of N atom in the ZnO crystal system.[18] The broaden peak appeared at frequency values of 3100–3600 cm^{-1} attributed to stretching vibrational peak of surface adsorbed O–H molecules. The co-doped ZnO FTIR spectrum consists of all vibrational peaks related to Gd/ZnO and N/ZnO nanoparticles. From the FTIR spectrum, it can be concluded that all elements are presented in the prepared nanoparticles have chemically interacted with ZnO nanoparticle.

3.3. UV-Vis-DRS and PL analysis

Optical absorption behaviour of the synthesized photocatalysts was studied with the help of UV-Vis-DRS spectrum and is demonstrated in Fig. 3. Bare ZnO shows the absorption wavelength of 396 nm with energy-gap of 3.13 eV. The absorption wavelength of Gd doped ZnO shows a slight blue shift compared to pure ZnO. The Gd/ZnO nanoparticle exhibits the cut-off wavelength of 392 nm with energy-gap of 3.16 eV. This blue shift revealed the reduction of crystallization and quantum confinement effect. The higher electronic population during the Gd doping in ZnO leads to the quantum confinement effect and blue shift in optical absorption behaviour.[12,16] The UV-Vis-DRS absorption spectrum of N doped ZnO shows the redshift with a cut-off wavelength of 406 nm. This redshift credited to electronic state alteration in ZnO crystal system owing to the existence of N atom. Comparatively high 2p π-electrons in N atom creating the sub-energy level in ZnO between the conduction and valance band. This leads to visible light absorption at N doped ZnO nanoparticle.[19] The calculated bandgap energy of N/ZnO was 3.05 eV. The co-doped ZnO nanoparticle shows the absorption wavelength of 401 nm with a bandgap of 3.09 eV. Hence, one could conclude that Gd and N doping can change the electronic level and boost the light absorption capability of co-doped ZnO nanoparticle.

Charge carriers recombination rate of the pure and doped ZnO nanoparticles during the photon illumination was analysed by photoluminescence spectrum with an excitation wavelength of 320 nm at room temperature and the outcomes were shown in Fig. 4. The PL spectrum demonstrated that the higher intensity attributed to fast charge carriers recombination, whereas the low intensity reveals the slow electron–hole recombination. The emission spectrum positioned at 388 nm attributed to charge carriers recombination at ZnO nanoparticle.[19] Compared to pure, Gd, and N doped ZnO, the Gd/N/ZnO nanoparticle exhibits lower emission peak intensity. This result implies that the Gd and N doping help to suppress the electron–hole recombination and it is beneficial to enhance the photocatalytic performance.

3.4. FESEM and TEM analysis

The apparent morphologies of the synthesized photocatalysts were recognized by FESEM analysis and the recorded micrographs were displayed in Fig. 5(a–d). From FESEM images, it could be verified that the prepared pure and doped ZnO nanoparticles have the spherical like morphology with extremely agglomerated particles. The surface morphology of the Gd, N and Gd/N doped ZnO remains constant as that of pure ZnO nanoparticle. This result revealed that the doping atom does not affect the morphology of the particles. The existence of all atoms and the distribution of the elements of Gd/N/ZnO nanoparticle was investigated by EDS analysis and the images are depicted in Fig. 6. The elemental distribution and EDS spectrum show the presence of Zn, Gd, N and O atoms in the synthesised Gd/N co-doped ZnO nanoparticle and elements are uniformly distributed on the photocatalyst surface.

In additional, the morphology and particle size of the Gd/N/ZnO nanoparticle was studied by TEM spectroscopy and the images are exposed in Fig. 7(a and b). TEM image of the Gd/N/ZnO nanoparticle shows the various sizes (30–60 nm) of the agglomerated particle, which is well-matched with the FESEM micrographs. The high-resolution TEM micrograph of the Gd and N co-doped ZnO nanoparticle was displayed in Fig. 7(c). The lattice plane distance of 0.238 nm and 0.282 nm related to the diffraction plane (101) and (110) respectively. The SAED pattern of Gd/N/ZnO nanoparticle was shown in Fig. 7(d).

3.5. XPS analysis

The chemical structure and oxidation value of the elements existing in pure and Gd/N doped ZnO nanoparticles were examined by X-ray photoelectron spectroscopy and the results

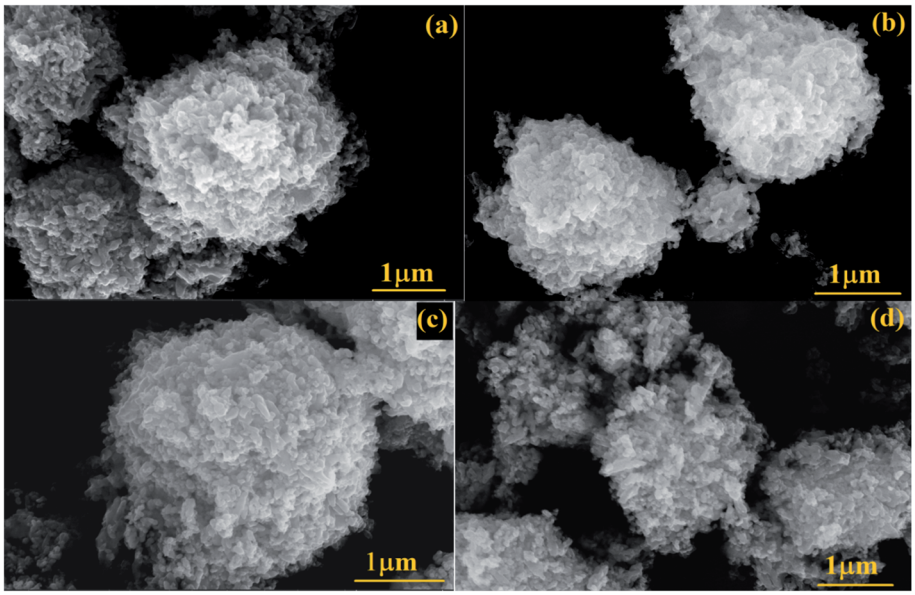

Fig. 5 FESEM images of (a) ZnO, (b) Gd/ZnO, (c) N/ZnO and (d) Gd/N/ZnO nanoparticles.

are shown in Fig. 8, S1 and S2.† The survey spectrum of pure and co-doped ZnO was depicted in Fig. S1.† The Gd/N/ZnO nanoparticle survey spectrum has consists of zinc, nitrogen, gadolinium and oxygen atoms and it is well-matched with the EDS elemental mapping. The high-resolution XPS spectrum of the co-doped ZnO nanoparticle was shown in Fig. 8. From Zn 2p HRXPS spectrum for Gd/N/ZnO, one can concluded that the peaks positioned at 1022.28 eV and 1045.98 eV allotted to Zn $2p_{3/2}$ and Zn $2p_{1/2}$ respectively. Whereas, the pure ZnO exhibit the Zn $2p_{3/2}$ and $2p_{1/2}$ peaks positioned at binding energy values of 1021.20 eV and 1044.27 eV, which is shown in Fig. S2.† From the XPS results, it can be clearly observed that Gd^{3+} doped ZnO

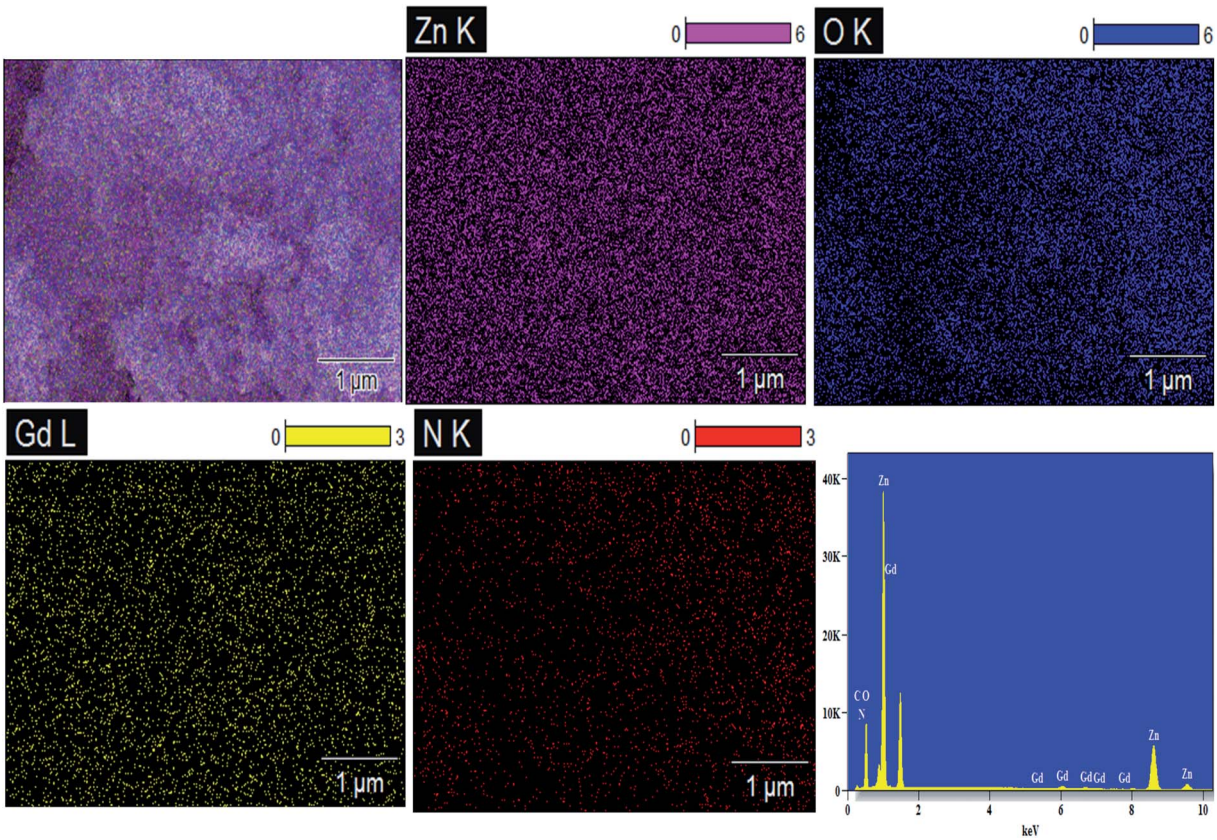

Fig. 6 EDS elemental distribution of Gd/N/ZnO nanoparticle.

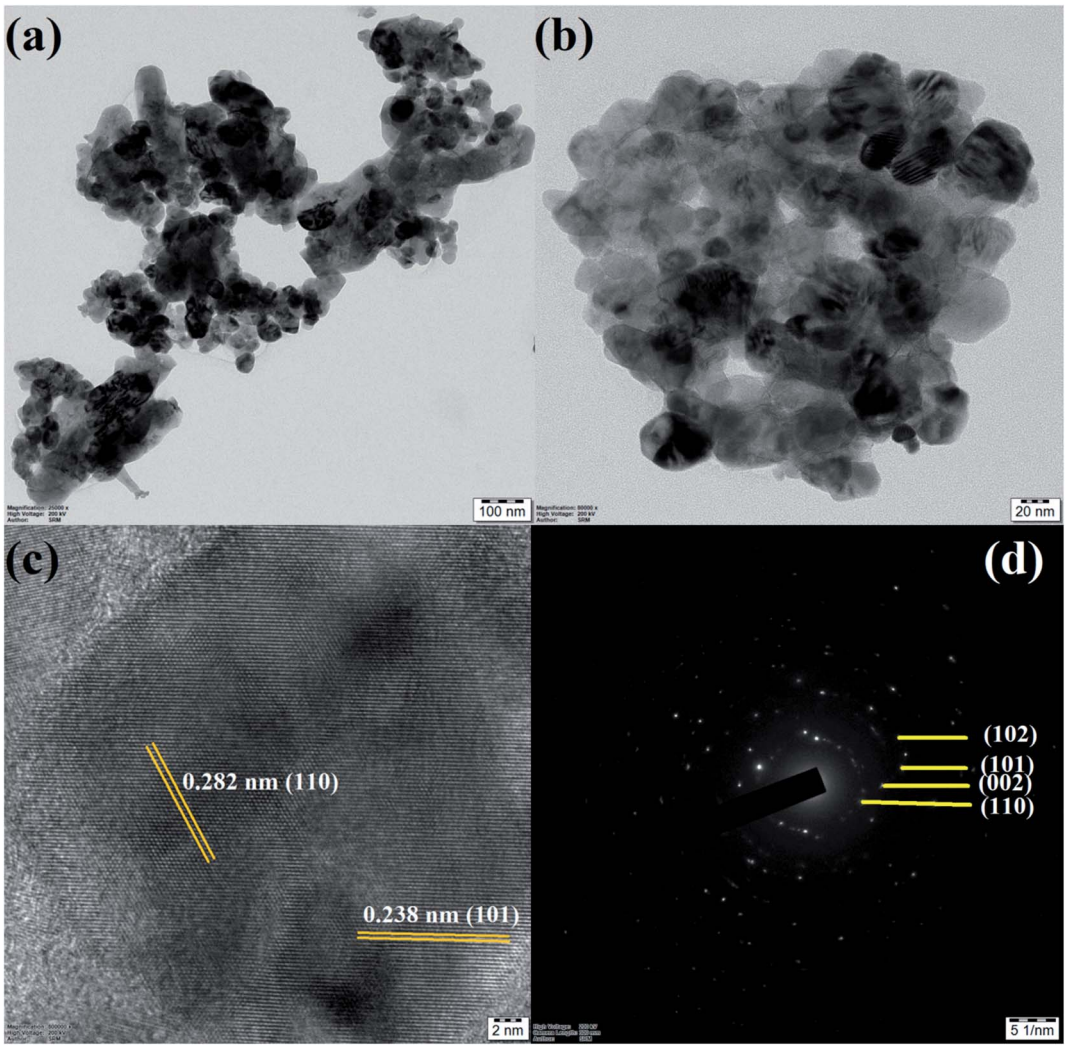

Fig. 7 (a and b) TEM, (c) HRTEM and (d) SAED pattern of Gd/N/ZnO nanoparticle.

have higher binding energy compared to pure ZnO. This binding energy shift demonstrated the Gd^{3+} ion replacement at Zn^{2+} crystal site.[34] The binding energy difference between Zn 2p peaks (23.7 eV) revealed that zinc has +2 oxidation states and it is compatible with the previous results.[13,20] The HRXPS spectrum of Gd 4d revealed the two characteristic peaks positioned at 140.78 eV and 143.88 eV related to the Gd $4d_{5/2}$ and Gd $4d_{3/2}$ respectively. The presence of these two deconvoluted peaks demonstrated that the Gd^{3+} oxidation state in prepared nanoparticle.[21] From the high resolution, N 1s XPS spectrum (Fig. 8(c)), the deconvoluted peaks 399.78 eV and 400.78 eV described the Zn–N bond and Zn–N–O bond respectively.[22] The high-resolution O 1s XPS spectrum was deconvoluted by three peaks which were positioned at 530.98, 532.18, and 533.58 eV were assigned to C–OH, Zn–O, and C=O bond respectively with O^{2-} oxidation state.[20] The pure ZnO also have three deconvoluted peaks positioned at 529.73, 530.63, and 531.08 eV. The observed O 1s peak shift demonstrated the Gd^{3+} and N doping greatly influence the chemical environmental between Zn and O atoms on the surface host lattice and the doping changes the ratio of chemisorbed oxygen.[34] Hence the XPS spectrum confirmed the presence of Zn, Gd, N and O elements in the prepared Gd/N/ZnO nanoparticle.

3.6. Photocatalytic analysis

To determine the photocatalytic behaviour of the prepared pure and doped ZnO nanoparticles was analysed by MB dye degradation under the UV-Vis and direct solar light irradiation. The obtained degradation results and their kinetic values are displayed in Fig. 9. The dye solution was magnetically stirred in the dark condition to reach the adsorption–desorption between the surface of the photocatalyst and dye solution. From the degradation result, it could be observed that after the light irradiation the Mb dye gets degraded. This outcome confirmed the removal of MB is chiefly due to the photocatalytic degradation. Likewise, the photolysis process confirmed the constancy of the MB dye molecule in the absence of light radiance. Under the UV-Vis light irradiation, the MB dye degraded up to 22% using pure ZnO nanoparticle, which is comparatively lower than Gd/ZnO (47%) and N/ZnO (63%) photocatalysts. This outcome

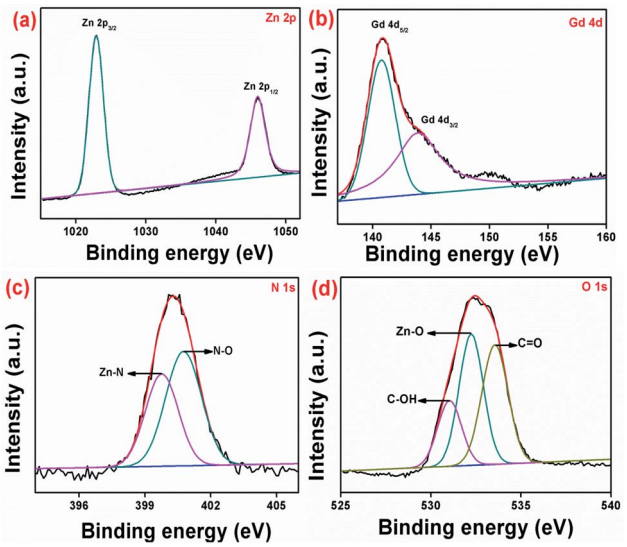

Fig. 8 High resolution XPS spectrum of Gd/N/ZnO nanoparticle (a) Zn 2p, (b) Gd 4d, (c) N 1s and (d) O 1s.

confirmed that the photocatalytic degradation effectiveness of the ZnO photocatalyst was considerably upgraded by Gd and N doping. The calculated MB degradation efficiency of Gd/N/ZnO nanoparticle was 87% after 60 min of UV-Vis light irradiation. The improved degradation effectiveness of the doped nanoparticles compared to pure ZnO credited to active light absorption performance and destruction of photo-induced charge carriers recombination. To govern the reaction rate constant for MB dye degradation under UV-Vis light radiation, pseudo-first-order kinetic relation was used and the results are exposed in Fig. 9(b). The pseudo 1st order kinetic relation is as follow[23–26]

$$\mathrm{Ln}(C/C_0) = -kt$$

where C_0 and C refer to the dye concentration at initial and irradiation time. The term 'k' refers to the kinetic rate constant.

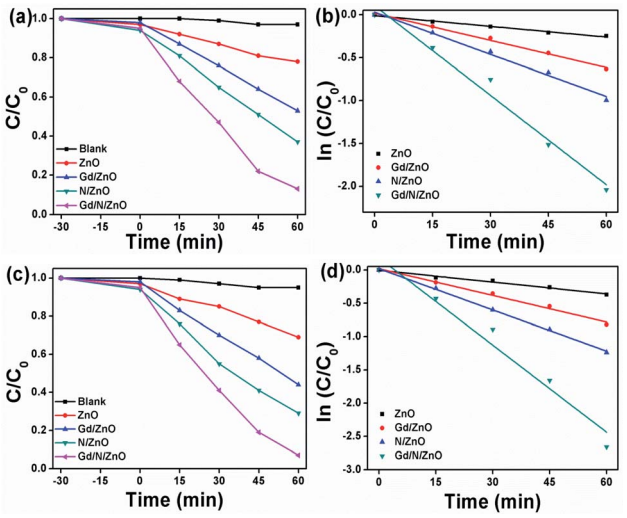

Fig. 9 MB dye degradation and pseudo 1st order rate constant values; (a and b) UV-Vis and (c and d) solar light.

The calculated rate constant for MB dye degradation under UV-Vis light irradiation was 0.004, 0.01, 0.016 and 0.034 min^{-1} for pure, Gd, N and Gd/N co-doped ZnO nanoparticles respectively.

Further, the MB dye degradation was performed under direct sunlight irradiation using prepared ZnO nanoparticles and the obtained results are shown in Fig. 9(c). The recorded degradation efficiency using pure ZnO nanoparticle was 31% after 60 min of light irradiation. The maximum MB degradation values of 56%, 71%, and 93% obtained using Gd/ZnO, N/ZnO, and Gd/N/ZnO respectively. Compared to UV-Vis light, the direct sunlight can degrade the MB more effectively. This is mainly attributed to the relatively high reaction temperature and high-intensity light.[27] The calculated kinetic rate constant for MB dye degradation using Gd/N/ZnO was 0.027 min^{-1}, which is 3.3 and 2 times higher than the Gd/ZnO and N/ZnO respectively. Hence, it can be concluded that the synthesized photocatalytsts were valuable for the real application to waste water contaminant degradation under the illumination of sunlight.

In order to determine the reactive oxygen species for the MB degradation, the elemental trapping experiment was performed in the UV-Vis light irradiation and the results are displayed in Fig. 10. To confirm the production of holes (h^+), superoxide (O_2^-) radical, and hydroxyl radical, EDTA (ethylenediaminetetraacetic acid disodium), BQ (benzoquinone) and IPA (isopropanol) were used. From elemental trapping results (Fig. 10), it could be detected that the addition of BQ greatly reduces the MB degradation efficiency and IPA plays a secondary role in the photocatalytic reaction. This result verified the superoxide and hydroxyl radicals are the main active element for photocatalytic degradation reaction. The addition of EDTA does not affect the degradation reaction.

From the above-mentioned trapping test, we have suggested the possible reaction mechanism for MB dye degradation reaction under photon irradiation. The conduction and valance band potential of the prepared Gd and N co-doped ZnO nanoparticle was calculated using the following relation[27–31]

$$E_{CB} = \chi - E_e - 0.5E_g$$

$$E_{VB} = E_{CB} + E_g$$

where, χ, E_e and E_g signify the electronegativity, electron energy in hydrogen scale (4.5 eV), and energygap of the photocatalyst. The calculated CB and VB values are −0.2 V (in V *vs.* NHE) and 2.89 V for Gd/N/ZnO nanoparticle.

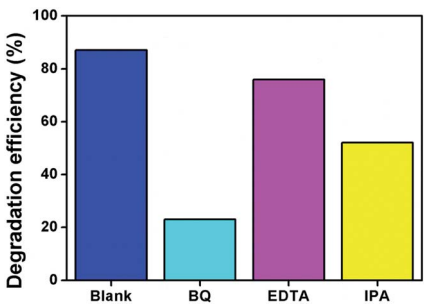

Fig. 10 Elemental trapping experiment using Gd/N/ZnO nanoparticle.

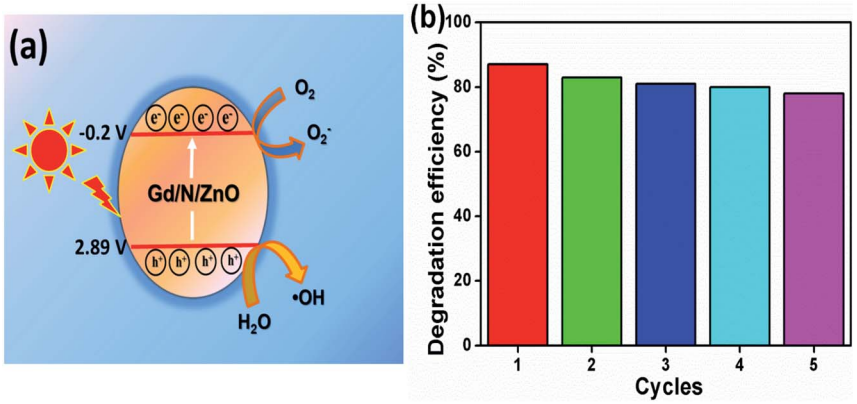

Fig. 11 (a) Possible reaction mechanism and (b) recycle test.

Table 1 Comparison between previous and present work

Sample	Dye	Irradiation time (min)	Light source	DE (%)	References
Gd,Nd co-doped ZnO	MB	120	300 W tungsten lamp	93	5
La (Sm) doped ZnO	MB	200	Sunlight	62 (60)	6
PVP capped Gd doped ZnO	MO	90	160 W UV bulb	82.89	8
N doped ZnO	MB	80	250 W UV light	98.6	18
ZnO	MB	180	250 W Hg lamp	99	32
ZnO	MB	150	250 W Hg lamp	95	33
Gd,N co-doped ZnO	MB	60	300 W halogen (sunlight)	87 (93)	This work

The possible reaction mechanism of Gd/N/ZnO was shown in Fig. 11(a). When the photons are illuminated on the surface of the nanoparticles the valance band (VB) electrons get excited and travelled to the conduction band (CB). These electrons are trapped by the sub-energy level created by the Gd and N doping to ZnO crystal system. The doping of heteroatom can alter the electronic arrangement of the photocatalyst and it eliminates the limitation of the narrowed light usage. The metal atom doping generates the sub-energy level under the CB, whereas N doping produces the sub-energy level above the VB. These sub-energy levels help to inhibit the excited electron–hole recombination. In this way, the formed conduction band electrons and valance band holes initiates the reduction and oxidation reactions respectively. The produced superoxide radicals by the reduction reaction combine with hydroxyl radicals and it generated the H_2O_2, which further produces the $OH^{\bullet}$ radicals. The produced hydroxyl radicals can degrade the dye molecule. The probable reaction mechanism for the MB dye degradation process

$$\text{Gd/N/ZnO} + h\nu \rightarrow \text{ZnO}\ (e^-/h^+)$$

$$\text{Gd/N/ZnO}\ (h^+) + H_2O \rightarrow {}^{\bullet}OH\cdot + H^+$$

$$\text{Gd/N/ZnO}\ (e^-) + O_2 \rightarrow O_2^-$$

$$O_2^- + H^+ + e^- \rightarrow OH^- + {}^{\bullet}OH\cdot$$

$${}^{\bullet}OH\cdot + \text{dye} \rightarrow \text{intermediate products}$$

In order to check the stability of the synthesized photocatalyst, the recycling experiment was performed under UV-Vis light irradiation and the results are shown in Fig. 11(b). Five consecutive recycles were completed for MB dye degradation using Gd/N/ZnO nanoparticle. The photocatalyst was recovered by ultra-centrifuge process and it was washed with acetone and de-ionized water for three times. Then the recovered sample was dried at 60 °C for 1 h to use the further cycles. For each recycling process, some amount of fresh photocatalyst was added to compensate for the loss (~15 wt%) during the recycling process. From the reusing experiment, it can be concluded that the Gd/N/ZnO nanoparticle have the high stability and it is valuable for the organic pollutant degradation reaction. Furthermore, the produced photocatalysts reveals the outstanding photocatalytic degradation efficiency compared to the previous results and the comparison table was shown in Table 1.

4. Conclusion

In summary, the facile wet-chemical co-precipitation method was used to prepare the Gd and N co-doped ZnO nanoparticle. The foreign ion doping enhances the light absorption ability and suppresses the charge carrier's recombination, which is confirmed by UV-Vis-DRS and PL analysis respectively. The co-doped ZnO nanoparticle exhibited better photocatalytic degradation efficiency under UV-Vis and direct solar light irradiation. The superoxide and hydroxyl radicals play a key role in the degradation reaction. Besides, the prepared photocatalyst

showed excellent recycling stability, which is beneficial for the practical application. Hence, the presented reports demonstrated that Gd/N/ZnO could be promising photocatalyst for environmental remediation application.

Conflicts of interest

There are no conflicts to declare.

Acknowledgements

The authors extend their appreciation to the Deanship of Scientific Research at King Saud University for funding this work through the research group no. RGP-1441-305.

References

1 A. Phuruangrat, S. Thongtem and T. Thongtem, Synthesis and characterization of Gd-doped PbMoO4 nanoparticles used for UV-lightdriven photocatalysis, *J. Rare Earths*, 2020.
2 U. Alam, A. Khan, a D. Ali, D. Bahnemann and M. Muneer, Comparative photocatalytic activity of sol–gel derived rare earth metal (La, Nd, Sm and Dy)-doped ZnO photocatalysts for degradation of dyes, *RSC Adv.*, 2018, **8**, 17582–17594.
3 P. Kalisamy, M. Lallimathi, M. Suryamathi, B. Palanivel and M. Venkatachalam, ZnO-embedded S-doped g-C3N4 heterojunction: mediator-free Z-scheme mechanism for enhanced charge separation and photocatalytic degradation, *RSC Adv.*, 2020, **10**, 28365–28375.
4 R. Bomila, S. Suresh and S. Srinivasan, Synthesis, characterization and comparative studies of dual doped ZnO nanoparticles for photocatalytic applications, *J. Mater. Sci.: Mater. Electron.*, 2019, **30**, 582–592.
5 J. Akhtar, M. B. Tahir, M. Sagir and H. S. Bamufleh, Improved photocatalytic performance of Gd and Nd co-doped ZnO nanorods for the degradation of methylene blue, *Ceram. Int.*, 2020, **46**, 11955–11961.
6 D. Ali, M. Z. Butt, I. Muneer, M. A. Farrukh, M. Aftab, M. Saleem, F. Bashir and A. U. Khan, Synthesis and characterization of sol-gel derived La and Sm doped ZnO thin films: A solar light photo catalyst for methylene blue, *Thin Solid Films*, 2019, **679**, 86–98.
7 K. Ahmad Malik, J. H. Malik, A. A. Bhat, I. Assadullah and R. Tomar, Trap assisted visible light luminescent properties of hydrothermally grown Gd doped ZnO nanostructures, *Vacuum*, 2021, **183**, 109832.
8 R. Dhir, Photocatalytic degradation of methyl orange dye under UV irradiation in the presence of synthesized PVP capped pure and gadolinium doped ZnO nanoparticles, *Chem. Phys. Lett.*, 2020, **746**, 137302.
9 N. K. Divya and P. P. Pradyumnan, High dielectric constant, low loss and high photocatalytic activity in Gd doped ZnO systems, *Mater. Res. Express*, 2017, **4**, 015904.
10 M. Faraz, F. Naqvi, M. Shakira and N. Khare, Synthesis of samarium-doped zinc oxide nanoparticles with improved photocatalytic performance and recyclability under visible light irradiation, *New J. Chem.*, 2018, **42**, 2295–2305.
11 O. Yayapao, T. Thongtem, A. Phuruangrat and S. Thongtem, Synthesis and characterization of highly efficient Gd doped ZnO photocatalyst irradiated with ultraviolet and visible radiations, *Mater. Sci. Semicond. Process.*, 2015, **39**, 786–792.
12 S. Selvaraj, M. Krishna Mohan, M. Navaneethanb, S. Ponnusamy and C. Muthamizhchelvan, Synthesis and photocatalytic activity of Gd doped ZnO nanoparticles for enhanced degradation of methylene blue under visible light, *Mater. Sci. Semicond. Process.*, 2019, **103**, 104622.
13 R. Gupta, N. K. R. Eswar, J. M. Modak and G. Madras, Visible light driven efficient N and Cu co-doped ZnO for photoinactivation of Escherichia coli, *RSC Adv.*, 2016, **6**, 85675–85687.
14 M. Dhonde, K. Sahu, V. V. S. Murty, S. Sankar Nemala, P. Bhargava and S. Mallick, Enhanced photovoltaic performance of a dye sensitized solar cell with Cu/N Co-doped TiO2 nanoparticles, *J. Mater. Sci.: Mater. Electron.*, 2018, **29**, 6274–6282.
15 B. Palanivel, M. Shkir, T. Alshahrani and A. Mani, Novel NiFe2O4 deposited S-doped g-C3N4 nanorod: Visible-light-driven heterojunction for photo-Fenton like tetracycline degradation, *Diamond Relat. Mater.*, 2020, 108148.
16 B. Palanivel and A. Mani, Conversion of a Type-II to a Z-Scheme Heterojunction bycIntercalation of a 0D Electron Mediator between the Integrative NiFe2O4/g-C3N4 Composite Nanoparticles: Boosting the Radical Production for Photo-Fenton Degradation, *ACS Omega*, 2020, **5**, 19747–19759.
17 N. Farhadian, R. Akbarzadeh, M. Pirsaheb, T.-C. Jen, Y. Fakhri and A. Asadi, Chitosan modified N, S-doped TiO2 and N, S-doped ZnO for visible light photocatalytic degradation of tetracycline, *Int. J. Biol. Macromol.*, 2019, **132**, 360–373.
18 E. Prabakaran and K. Pillay, Synthesis of N-doped ZnO nanoparticles with cabbage morphology as a catalyst for the efficient photocatalytic degradation of methylene blue under UV and visible light, *RSC Adv.*, 2019, **9**, 7509–7535.
19 C. N. Peter, W. W. Anku, R. Sharma, G. M. Joshi, S. K. Shukla and P. P. Govender, N-doped ZnO/graphene oxide: a photostable photocatalyst for improved mineralization and photodegradation of organic dye under visible light, *Ionics*, 2019, **25**, 327–339.
20 P. Thirukumaran, R. Atchudan, A. S. Parveen, K. Kalaiarasan, Y. R. Lee and S.-C. Kim, Fabrication of ZnO nanoparticles adorned nitrogen-doped carbon balls and their application in photodegradation of organic dyes, *Sci. Rep.*, 2019, **9**, 19509.
21 N. Zhang, D. Chen, F. Niu, S. Wang, L. Qin and Y. Huang, Enhanced visible light photocatalytic activity of Gd doped BiFeO3 nanoparticles and mechanism insight, *Sci. Rep.*, 2016, **6**, 26467.
22 H. Sudrajat and S. Babel, A novel visible light active N-doped ZnO for photocatalyticdegradation of dyes, *J. Water Process. Eng.*, 2017, **16**, 309–318.
23 B. Palanivel and M. Alagiri, Construction of rGO Supported Integrative NiFe2O4/g-C3N4 Nanocomposite: Role of Charge Transfer for Boosting the OH. Radical Production

to Enhance the Photo-Fenton Degradation, *ChemistrySelect*, 2020, **5**, 9765–9775.

24 M. Lallimathi, P. Kalisamy, M. Suryamathi, T. Alshahrani, M. Shkir, M. Venkatachalam and B. Palanivel, Carbon Dot Loaded Integrative CoFe2O4/g-C3N4 P-N Heterojunction: Direct Solar Light-Driven Photocatalytic H2 Evolution and Organic Pollutant Degradation, *ChemistrySelect*, 2020, **5**, 10607–10617.

25 B. Palanivel, T. Maiyalagan, J. Venkatesan, C. Ayyappan and M. Alagiri, Rational design of ZnFe2O4/g-C3N4 nanocomposite for enhanced photo-Fenton reaction and supercapacitor performance, *Appl. Surf. Sci.*, 2019, **498**, 143807.

26 B. Palanivel, V. Jayaraman, C. Ayyappan and M. Alagiri, Magnetic binary metal oxide intercalated g-C3N4: Energy band tuned pn heterojunction towards Z-scheme photo-Fenton phenol reduction and mixed dye degradation, *J. Water Process. Eng.*, 2019, **32**, 100968.

27 B. Palanivel, C. Ayappan, V. Jayaraman, S. Chidambaram, R. Maheswaran and A. Mani, Inverse spinel NiFe2O4 deposited g-C3N4 nanosheet for enhanced visible light photocatalytic activity, *Mater. Sci. Semicond. Process.*, 2019, **100**, 87–97.

28 P. Matheswaran, P. Thangavelu and B. Palanivel, Carbon dot sensitized integrative g-C3N4/AgCl Hybrids: An synergetic interaction for enhanced visible light driven photocatalytic process, *Adv. Powder Technol.*, 2019, **30**, 1715–1723.

29 B. Palanivel, M. Lallimathi, B. Arjunkumar, M. Shkir, T. Alshahrani, K. S. Al-Namshah, M. S. Hamdy, S. Shanavas, M. Venkatachalam and G. Ramalingam, rGO supported g-C3N4/CoFe2O4 heterojunction: Visible-light-active photocatalyst for effective utilization of H2O2 to organic pollutant degradation and $OH^{\bullet}$ radicals production, *J. Environ. Chem. Eng.*, 2020, 104698.

30 F. A. Alharthi, A. A. Alghamdi, H. S. Alanazi, A. A. Alsyahi and N. Ahmad, Photocatalytic Degradation of the Light Sensitive Organic Dyes: Methylene Blue and Rose Bengal by Using Urea Derived g-C3N4/ZnO Nanocomposites, *Catalysts*, 2020, **10**, 1457.

31 F. A. Alharthi, A. A. Alghamdi, N. Al-Zaqri, H. S. Alanazi, A. A. Alsyahi, A. E. Marghany and N. Ahmad, Facile one-pot green synthesis of Ag–ZnO Nanocomposites using potato peel and their Ag concentration dependent photocatalytic properties, *Sci. Rep.*, 2020, **10**, 20229.

32 F. A. Alharthi, N. Al-Zaqri, A. E. marghany, A. A. Alghamdi, A. Q. Alorabi, N. Baghdadi, H. S. AL-Shehri, R. Wahab and N. Ahmad, Synthesis of nanocaulifower ZnO photocatalyst by potato waste and its photocatalytic efficiency against dye, *J. Mater. Sci.: Mater. Electron.*, 2020, **31**, 11538–11547.

33 F. A. Alharthi, A. A. Alghamdi, A. A. Alothman, Z. M. Almarhoon, M. F. Alsulaiman and N. Al-Zaqri, Green Synthesis of ZnO Nanostructures Using Salvadora Persica Leaf Extract: Applications for Photocatalytic Degradation of Methylene Blue Dye, *Crystals*, 2020, **10**, 441.

34 D. Ranjith Kumar, K. S. Ranjith and R. T. Rajendra Kumar, Structural, optical, photocurrent and solar driven photocatalytic properties of vertically aligned samarium doped ZnO nanorod arrays, *Optik*, 2018, **154**, 115–125.